Study of boundary layer separation over NACA 66_2-015 symmetric and cambered airfoil through numerical method

Mukund S
Undergraduate Student, Department of Mechanical Engineering,BMS College of Engineering, Banglore, 560078

Abstract

This case study aims to understand the flow over a symmetric and cambered airfoil in an incompressible flow condition. The primary objective of this case study is to study the boundary layer separation by varying the angle of attack. Further, the boundary layer separation is justified with the variation of coefficient of lift and drag values, as there will be a sudden drop in the coefficient of lift and rapid increase in the coefficient of drag due to stalling phenomena. k-ω SST turbulence model was utilized for solving this case and results were compared with the results obtained from ANSYS Fluent.

1. Introduction

Airfoils are two-dimensional wings also known as the infinite wing. It represents the cross-section of a finite wing. Airfoils are categorized based on their geometry and their use.

Based on the thickness of the camber, they are classified as,
i. Symmetric airfoil.
ii. Cambered airfoil.
These airfoils are further explained in the airfoil nomenclature.

Based on their use they are divided into three classes:
i. High lift
ii. General purpose
iii. High speed.

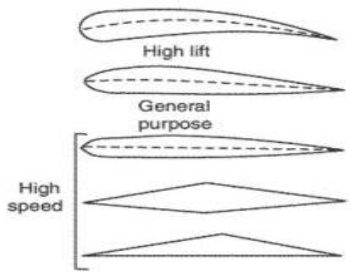

Fig. 1. Different airfoils[1]

High-lift aerofoil sections are normally used on sail planes and aircraft with short field operations. They have a high thickness chord ratio, a pronounced camber, and well-rounded leading edges. General purpose airfoil employ lower thickness to chord ratio, less camber and sharper trailing edges, and high speed section are used in high speed aircraft.[1]

Airfoil nomenclature

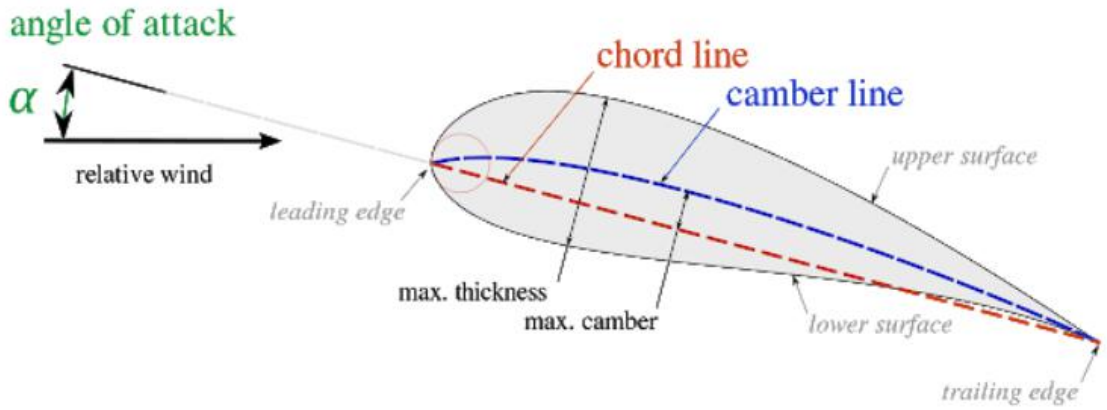

Fig. 2.Nomenclature of airfoil[2]

1. Leading edge - The leading edge of an airfoil surface such as a wing is its foremost edge and is therefore the part which first meets the oncoming air. It is also known as the higher pressure edge.

2. Trailing edge - The trailing edge of an aerodynamic surface such as a wing is its rear edge, where the airflow separated by the leading edge rejoins.

3. Chord line(c) - Straight line connecting the leading and trailing edge.

4. Mean/Camber line - The locus of points halfway between leading and trailing edge.

5. Camber - Maximum distance between mean camber line and chord line.

6. Angle of attack (alpha) - The angle the free stream velocity makes on the airfoil/vane. The angle is measured taking the chord line as reference.

Based on the camber thickness, airfoils are classified as symmetric and cambered. When the camber thickness is zero, the camber line and chord line are coincident, leading to a symmetric airfoil. If the camber line is off-set from the chord line, then airfoil is cambered.

A symmetric airfoil has zero lift at zero angle of attack, whereas a cambered airfoil has some significant lift at zero angle of attack. The angle of attack should be made negative for the lift to become zero for the cambered airfoil. This angle of attack is called the zero-lift angle of attack
As the angle of attack is increased, the value of lift increases along with the increase in drag value. This is due to the separation of the flow as the angle is increased. For symmetric airfoil, at zero angle of attack, there is very minimum flow separation and the pressure distribution on both sides of the airfoil is equal leading to no generation of lift. Whereas in the case of cambered airfoil there is flow separation at zero angle of attack leading to pressure differences in upper and lower surfaces of the wing hence, further leading to the generation of lift.
In this case study, the drag and lift values are compared for both, symmetric and cambered airfoils for various angles of attack and are presented in this report. The airfoils used for this case study is NACA 6 series airfoil. NACA 66_2-015 airfoil is used, both symmetric and cambered.

NACA has a standard way of representing the 6 series airfoil. These aerofoils are described using a series of digits following the word “NACA”.

The representation is

1st digit-Represents the series

2nd digit-Location of minimum pressure in tenths of chord from the leading edge.

3rd digit-Design lift coefficient in tenths

Last two digits-Thickness of the airfoil in hundredths of the chord.

This airfoil has 15% of the chord as its maximum thickness. Both the airfoil are shown below.

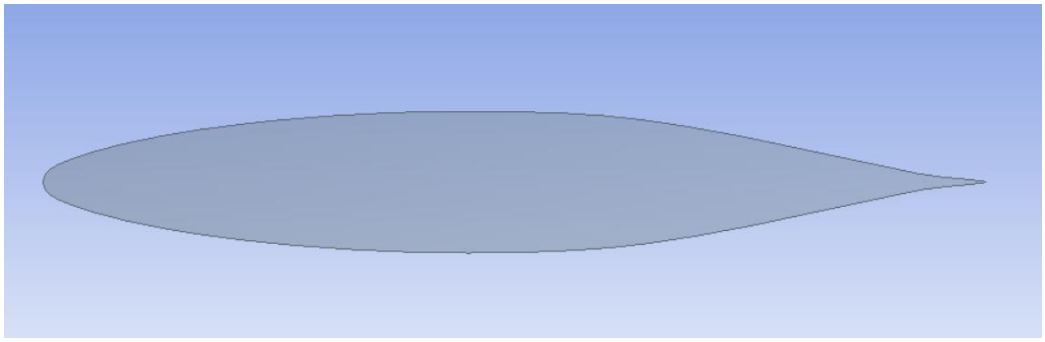

Fig. 3.NACA 66_2-015 symmetric airfoil

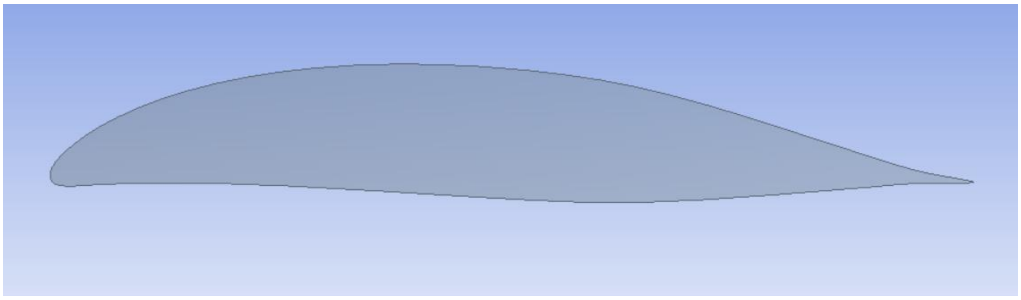

Fig. 4.NACA 66_2-015 cambered airfoil

The flow over the NACA 66(2)-015 was studied using Fluent in [9]. The current study aims to attempt a similar analysis using OpenFOAM

2. Problem Statement

CFD study on symmetric and cambered airfoils was conducted with the aid of OpenFOAM software. The particular airfoil used for this case study is NACA 66_2-015. The cambered model used for this case study is NACA $66_2$015 + Camber line Cl1 =1.0 at $\alpha = 4.56°$. The angle of attack is varied from 0^o to 16^o. C_L and C_D values will be determined. SimpleFoam solver is used for all the cases. Turbulence model used is k-ω SST, the turbulent energy (k)

and specific dissipation rate (ω) is determined by the following equation,

$$k=\frac{3}{2}(UI)^2 \quad (2.1)$$

$$\omega=\frac{\sqrt{k}}{l} \quad (2.2)$$

Pressure distribution and velocity contour is determined and compared with ANSYS Fluent results.

3. Governing Equations

The solver used for this case study is simpleFoam, it employs SIMPLE algorithm. The case study considered is a steady state, incompressible, three-dimensional flow. The set of Navier Stokes' equations governing the flow is given below.

The continuity equation is given as

$$\nabla.u=0 \quad (3.1)$$

The momentum equation is given as

$$\nabla\cdot(u\otimes u)-\nabla\cdot R=-\nabla p+Su \quad (3.2)$$

Where, u -velocity; p-kinematic pressure; R=stress tensor, Su=Momentum source

The discretized momentum equation and pressure correction equation are solved implicitly, where the velocity correction is solved explicitly. This is the reason why it is called "Semi-Implicit Method".

Turbulence Modelling

k-ω SST turbulence modelling is a two equation eddy viscosity turbulence model. SST stands for Shear Stress Transport, this model doesn't require any extra damping functions.

Kinematic eddy viscosity is given as,

$$\upsilon_T=\frac{a_1 k}{\max(a_1\omega, SF_2)} \quad (3.3)$$

Turbulent kinetic energy is given by,

$$\frac{\partial k}{\partial t}+U_j\frac{\partial k}{\partial x_j}=P_k-\beta^* k\omega+\frac{\partial}{\partial x_j}[(\nu+\sigma_k\nu_T)\frac{\partial k}{\partial x_j}] \quad (3.4)$$

Specific dissipation rate is given by,

$$\frac{\partial \omega}{\partial t} + U_j \frac{\partial \omega}{\partial x_j} = \alpha S^2 - \beta \omega^2 + \frac{\partial}{\partial x_j}[(\nu + \sigma_\omega \nu_T)\frac{\partial \omega}{\partial x_j}] + 2(1 - F_1)\sigma_{\omega 2} \frac{1}{\omega} \frac{\partial k}{\partial x_i} \frac{\partial \omega}{\partial x_i} \quad (3.5)$$

4. Simulation Procedure

4.1 Geometry and Mesh

Geometry creation

The airfoil used for this case study NACA 66_2-015. The geometrical data points were taken from "Theory of wing sections including a summary of airfoil data". Using appropriate formula the airfoil data points were created. It was later on uploaded to ANSYS design modeller and then the C-Domain was created, for both symmetric and cambered.

Computational Domain

The computational domain considered here is a C-Domain. The inlet taken is 8 times the length of the chord and the far-field is 16 times the length of the chord. The same domain is considered for both symmetric and cambered airfoils.

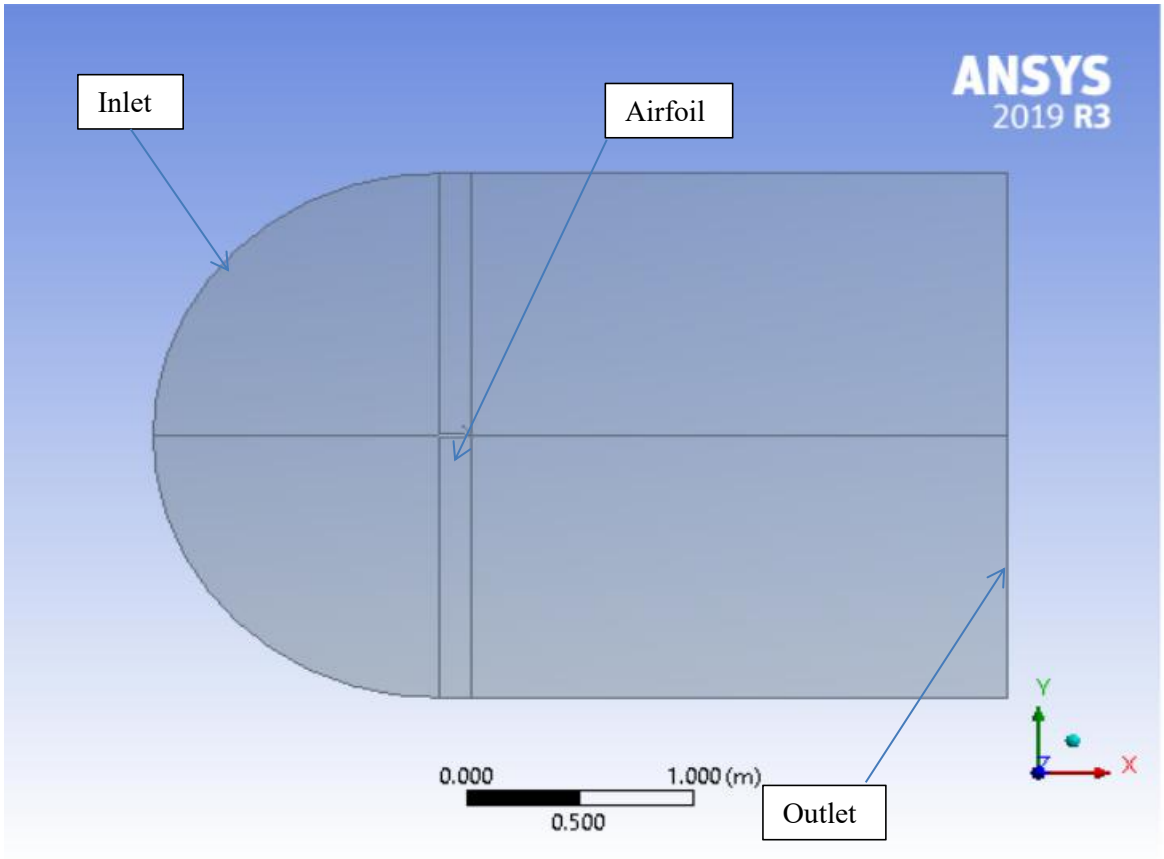

Fig. 5. Computational Domain

A mesh convergence study was conducted for symmetric airfoil with number of cells varying as 40k, 100k and 160k. The C-type structured grid with 160k quad elements is generated using ANSYS Fluent Meshing for symmetric airfoil. The enhanced wall treatment approach is used as the near-wall treatment method to resolve the near wall region including the viscous sub layer. The symmetric mesh is as shown in Fig. 6.

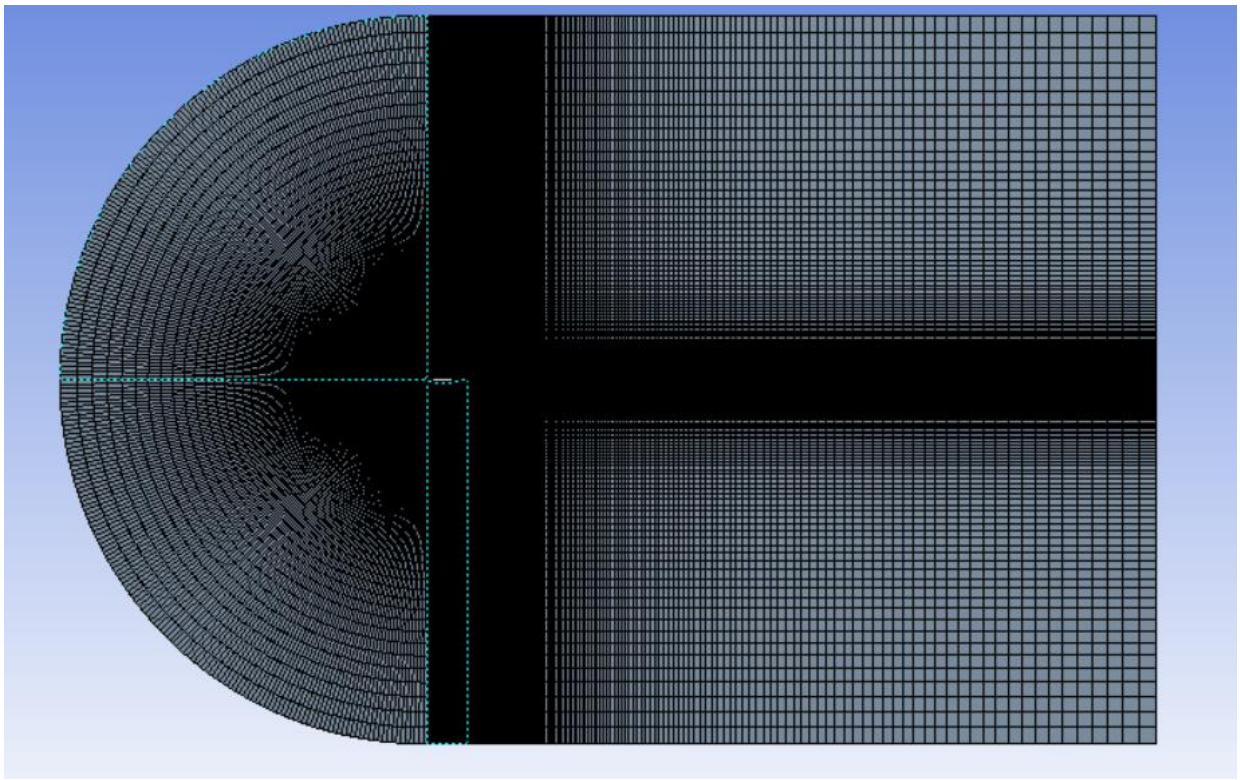

Fig. 6. Symmetric airfoil mesh

Similarly, a C-type structured grid with 40k quad elements is generated using ANSYS Fluent Meshing for cambered airfoil. The enhanced wall treatment approach is used as the near-wall treatment method to resolve the near wall region including the viscous sub layer. The cambered mesh is as shown in Fig. 7.

fluentMeshToFoam was used to convert the MESH file which was in ASCII format in .msh extension to foam format including multiple region and region boundary.

checkMesh command was used to check the validity of the mesh. Once this command is run, it gives back the information about the mesh quality and named sections. The symmetric mesh was fine, the cambered mesh had 35 non-orthogonal faces and it was written to set nonOrthoFaces.

4.2 Initial and Boundary Conditions

The simulation was conducted for an incompressible fluid conditions with the physical properties being as follows,

Density(kg/m^3)	1
Kinematic viscosity(m^2/s)	10^{-5}

Table. 1. Transport properties

The above information is stored in the transportProperties file in the constant folder.

The inlet and boundary conditions are store in the 0 folder. The variables of particular interest for k-ω SST turbulence modelling are turbulent kinetic energy(k), specific turbulent dissipation rate(ω), turbulent kinematic viscosity(nuT), pressure(p) and velocity(v).

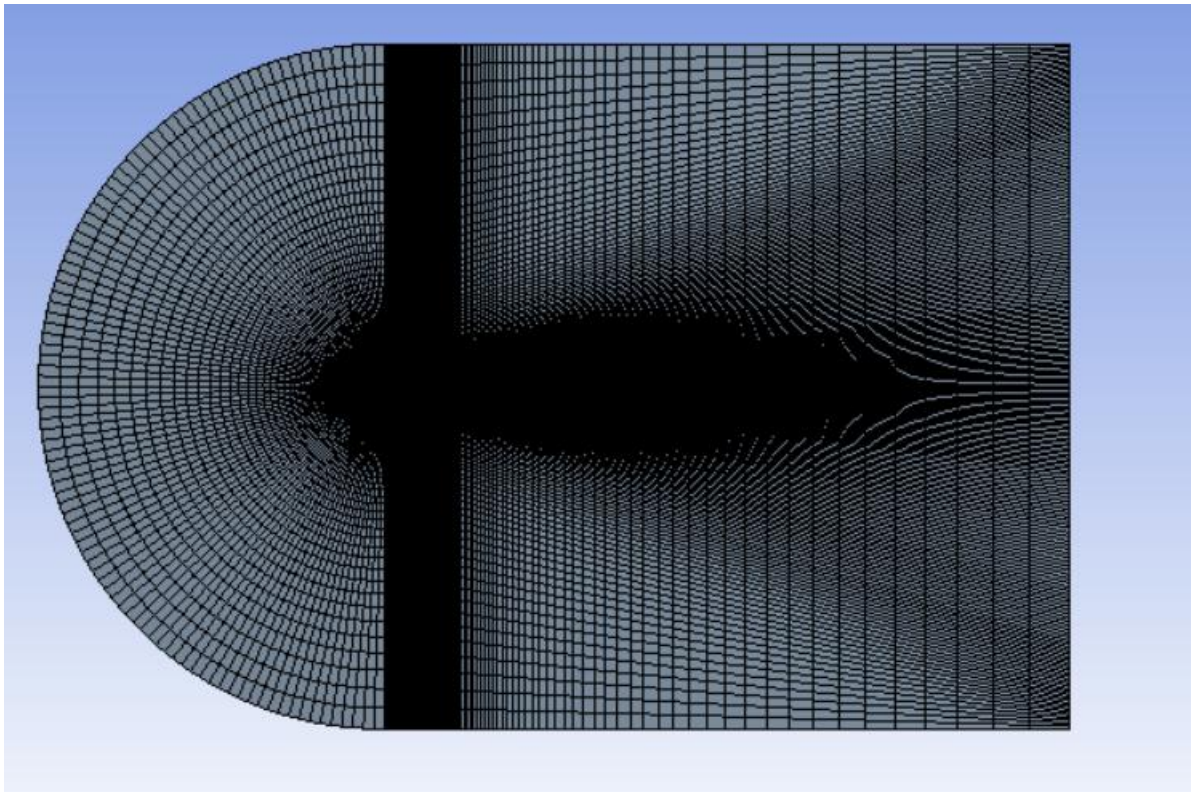

Fig. 7. Cambered airfoil mesh

The free stream conditions for the case study is given in the Table. 2. below,

Parameters	Values
Velocity	50 m/s
Pressure	0 Pa

Table. 2. Initial conditions

The angle of attack (AOA) was varied from 0^o to 16^o.

The boundary conditions used in the case study are summarised below in the Table. 3. Suitable

boundary conditions have been applied for the turbulent related terms, i.e, the wall functions are applied to the airfoil wall(Wall_surface_body).

Variable	Inlet	Outlet	Wall_surface_body	Frontand backpanels
Velocity(v)	freestreamVelocity	freestreamVelocity	fixedValue	empty
Pressure(p)	freestreamPressure	freestreamPressure	zeroGradient	empty
Turb K.E(k)	fixedValue	zeroGradient	kqRWallFunction	empty
Omega(ω)	fixedValue	zeroGradient	omegaWallFunction	empty
Turb viscosity(ν)	calculated	calculated	nutkWallFunction	empty

Table. 3. Boundary conditions

The turbulent properties, i.e. k and ω are determined from the below equations,

$$k=\frac{3}{2}(UI)^2 \tag{4.1}$$

$$\omega=\frac{\sqrt{k}}{l} \tag{4.2}$$

These values were determined as turbulent kinematic energy to be equal to 9.375 m^2/s^2 and specific dissipation as 62902.5 s^{-1}.

4.3 Solver

OpenFOAM or Open-source Field Operation And Manipulation is an open-source C++ tool used for solving continuum mechanics problems, mainly Computational-Fluid Dynamics(CFD) with a focus on Finite Volume Method (FVM). The software package includes solver codes for different kinds of transport phenomena, varying from simple laplacian solver called laplacianFoam to complex multiphase flow, compressible flow, heat transfer, incompressible flow, and many more. The flagship solver and most commonly used solver is simpleFoam. simpleFoam is a steady-state solver for incompressible, turbulent flow.

It utilizes the SIMPLE (Semi-Implicit Method for Pressure Linked Equations) algorithm. It is an approximation of the velocity field which is obtained by solving the momentum equation. The pressure gradient term is calculated using the pressure distribution from the previous iteration or an initial guess. The pressure equation is formulated and solved to obtain the new pressure distribution. Velocities are corrected and a new set of conservative fluxes is calculated.

5. Results and Discussions

A steady state simulation was carried out for each of the cases for 10000 iterations. k-ω SST turbulence modelling was used. The results of the simulations were visualized using ParaView by creating a ".foam" extension file. In ParaView the pressure and velocity distribution for the airfoils were visualized for varying angle of attack. The force coefficients were determined by writing a file to be calculated with every iteration.

The velocity and pressure contour plots were visualized for angle of attack varying from 0° to 16° keeping the free stream velocity as 50 m/s and the density of the fluid as 1 kg/m^3. These results are compared with the ones obtained from ANSYS Fluent. Apart from these contours, the lift and drag coefficients are also compared with that obtained from ANSYS Fluent.

The airfoil used is NACA 66$_2$-015 symmetric and cambered airfoil, the results are presented below.

The pressure distribution plots obtained for symmetric airfoil is presented below for both OpenFOAM and ANSYS.

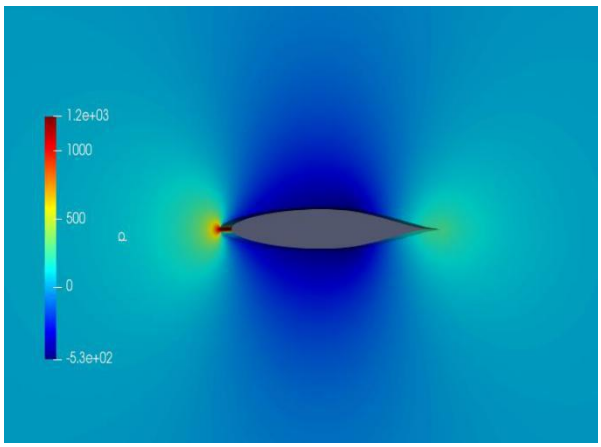

Fig. 8.a. 0° Symmetric airfoil pressure distribution(OpenFOAM)

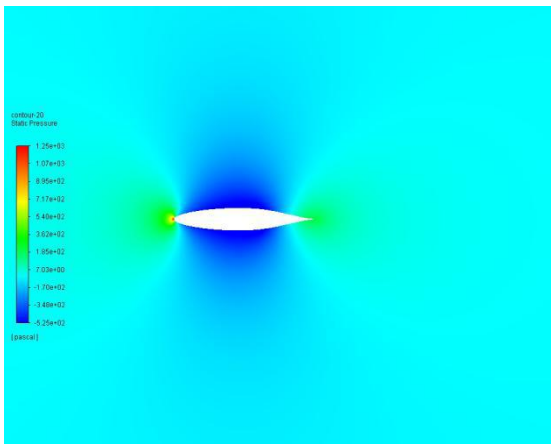

Fig. 8.b. 0° Symmetric airfoil pressure distribution(Fluent)

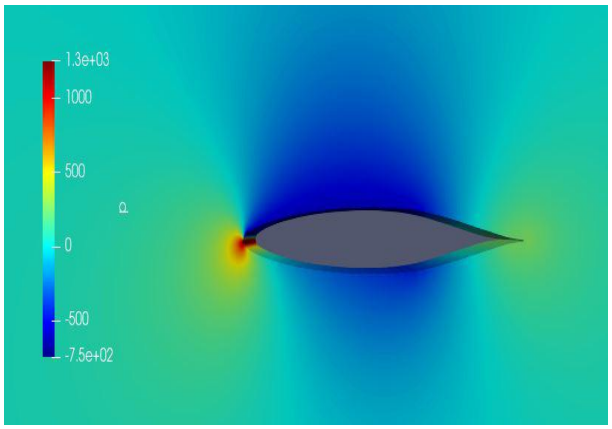

Fig. 9.a. 2º Symmetric airfoil pressure distribution(OpenFOAM)

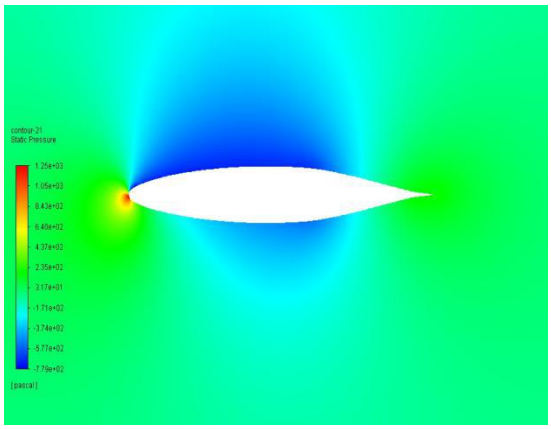

Fig. 9.b. 2º Symmetric airfoil pressure distribution(Fluent)

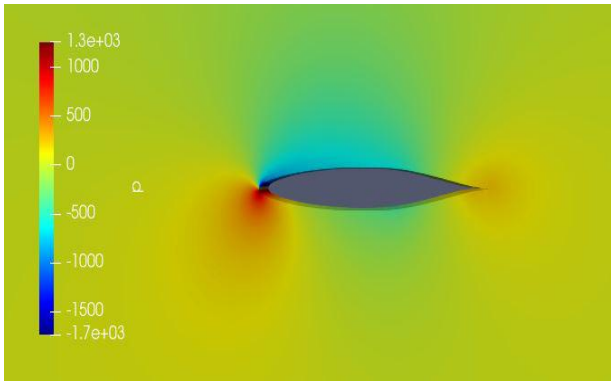

Fig. 10.a. 4º Symmetric airfoil pressure distribution(OpenFOAM)

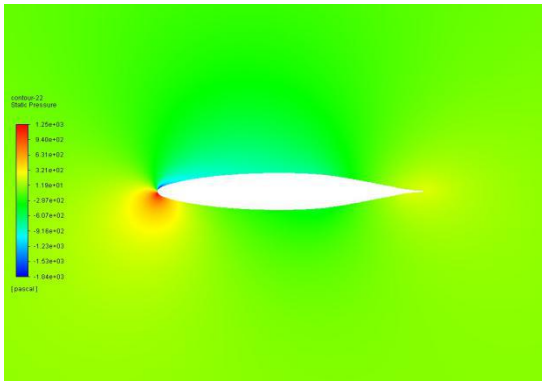

Fig. 10.b. 4º Symmetric airfoil pressure distribution(Fluent)

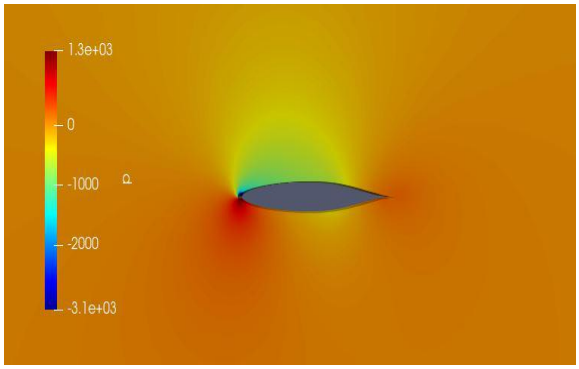

Fig. 11.a. 6º Symmetric airfoil pressure distribution(OpenFOAM)

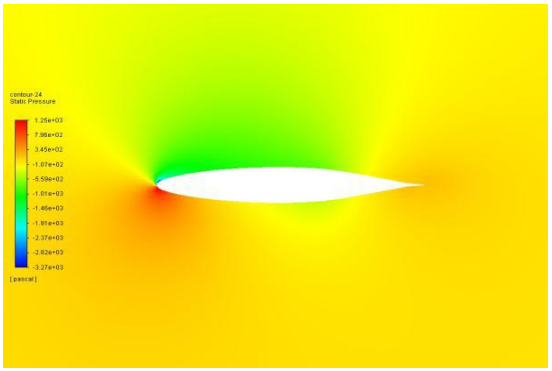

Fig. 11.a. 6º Symmetric airfoil pressure distribution(Fluent)

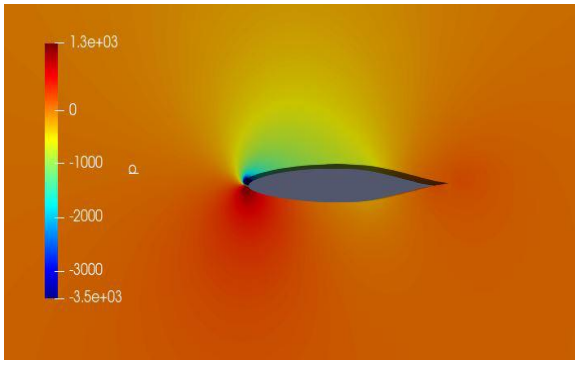

Fig. 12.a. 8º Symmetric airfoil pressure distribution(OpenFOAM)

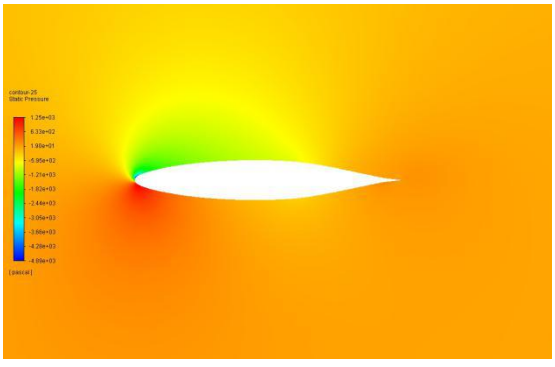

Fig. 12.b. 8º Symmetric airfoil pressure distribution(Fluent)

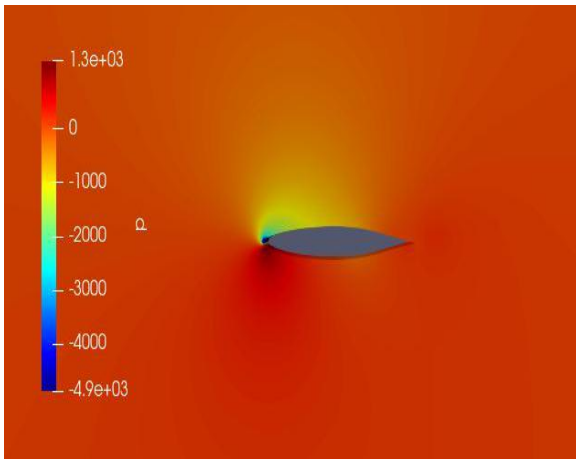

Fig. 13.a. 10º Symmetric airfoil pressure distribution(OpenFOAM)

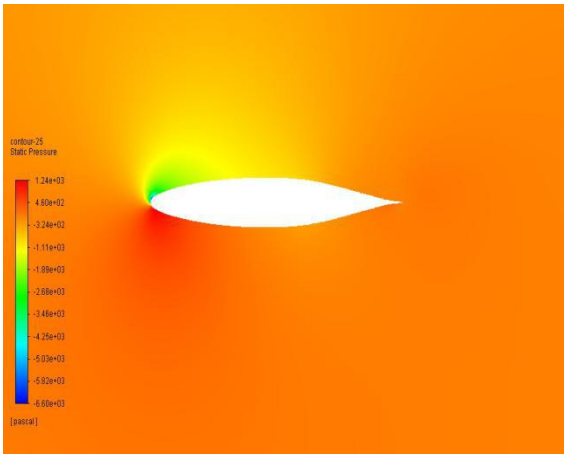

Fig. 13.b. 10º Symmetric airfoil pressure distribution(Fluent)

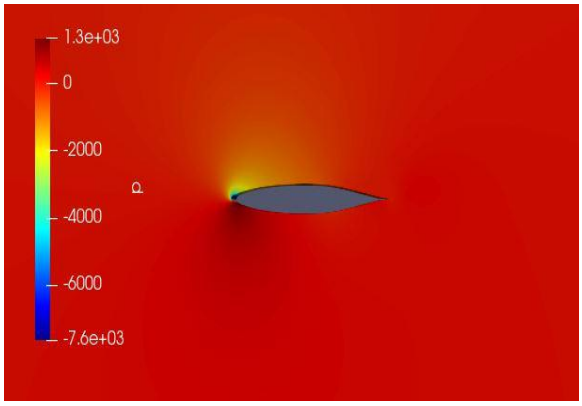

Fig. 14.a. 12º Symmetric airfoil pressure distribution(OpenFOAM)

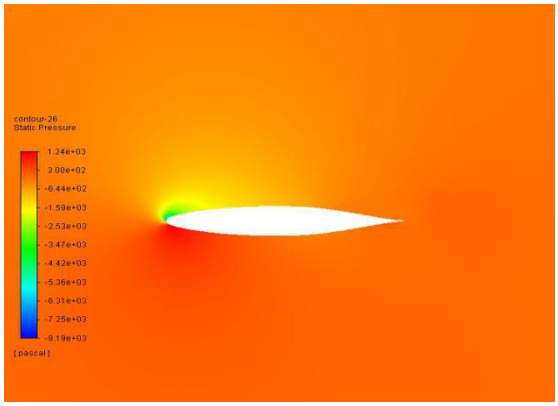

Fig. 14.b. 12º Symmetric airfoil pressure distribution(Fluent)

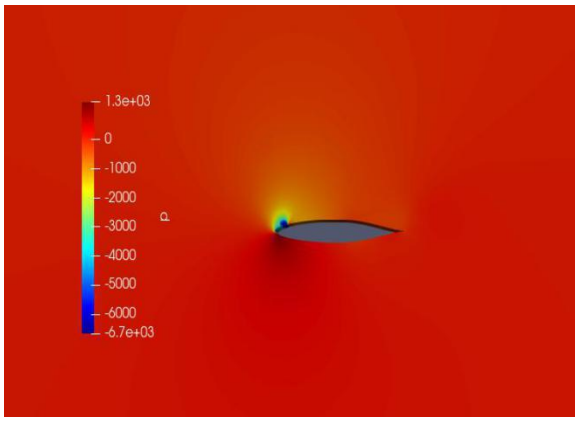

Fig. 15.a. 14º Symmetric airfoil pressure distribution(OpenFOAM)

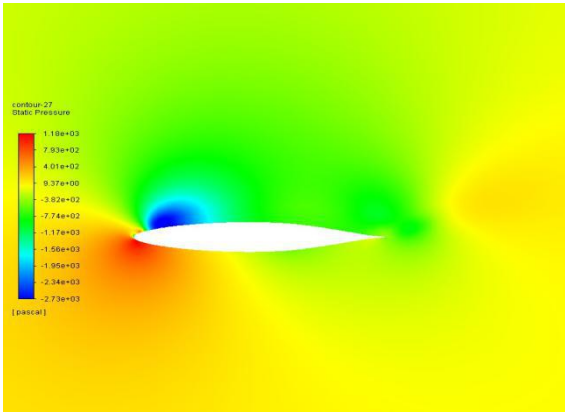

Fig. 15.b. 14º Symmetric airfoil pressure distribution(Fluent)

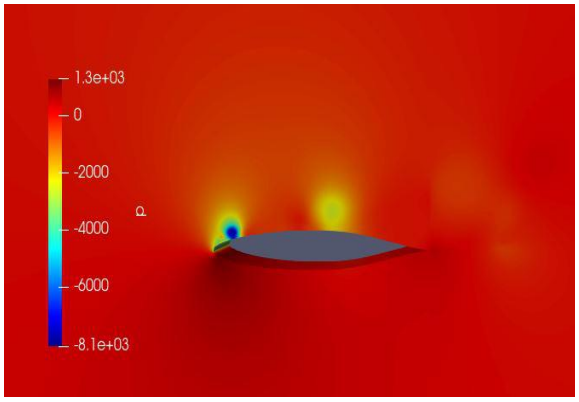

Fig. 16.a. 16º Symmetric airfoil pressure distribution(OpenFOAM)

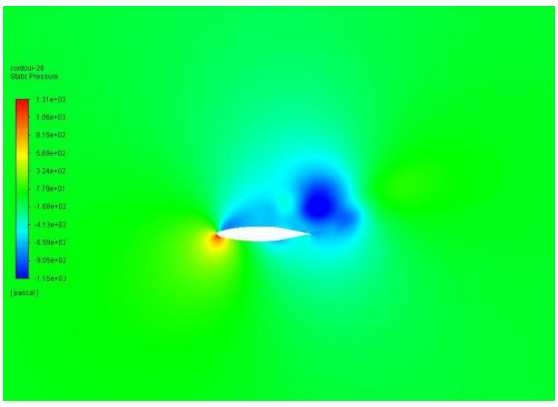

Fig. 16.b. 16º Symmetric airfoil pressure distribution(Fluent)

The velocity distribution plots obtained for symmetric airfoil is presented below for both OpenFOAM and ANSYS.

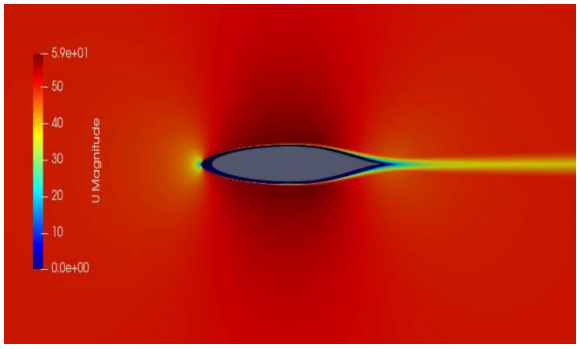

Fig. 17.a. 0º Symmetric airfoil velocity distribution(OpenFOAM)

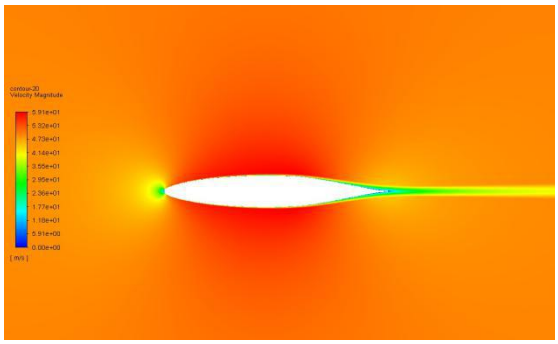

Fig. 17.b. 0º Symmetric airfoil velocity distribution(Fluent)

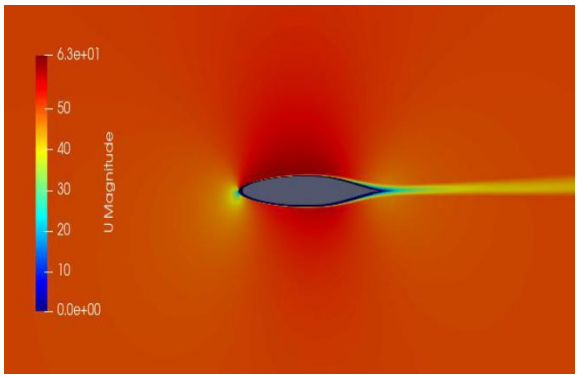

Fig. 18.a. 2º Symmetric airfoil velocity distribution(OpenFOAM)

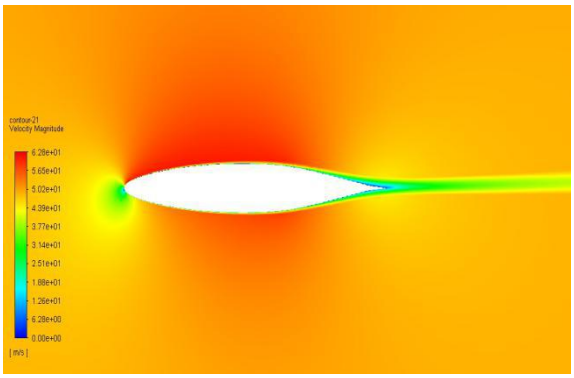

Fig. 18.b. 2º Symmetric airfoil velocity distribution(Fluent)

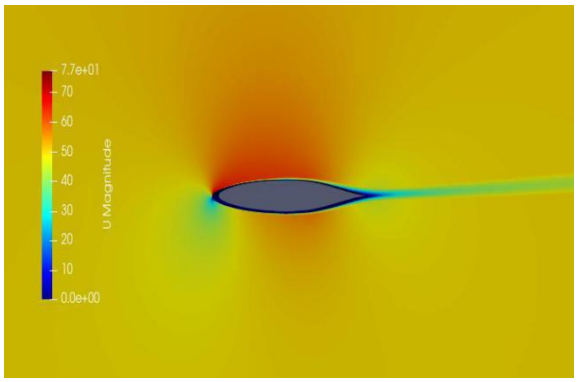

Fig. 19.a. 4º Symmetric airfoil velocity distribution(OpenFOAM)

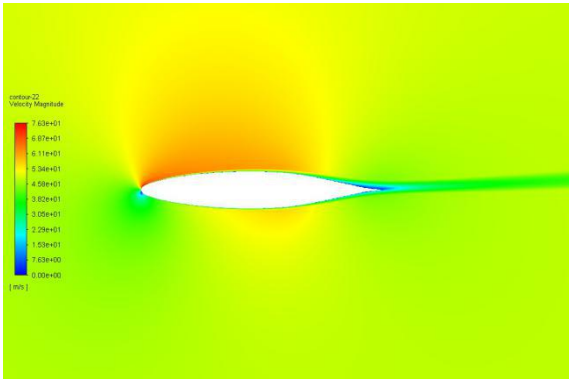

Fig. 19.b. 4º Symmetric airfoil velocity distribution(Fluent)

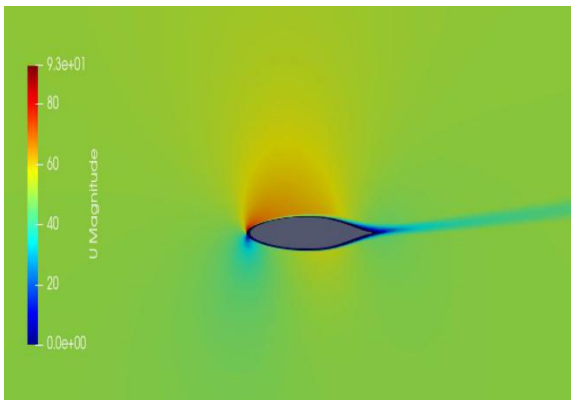

Fig. 20.a. 6º Symmetric airfoil velocity distribution(OpenFOAM)

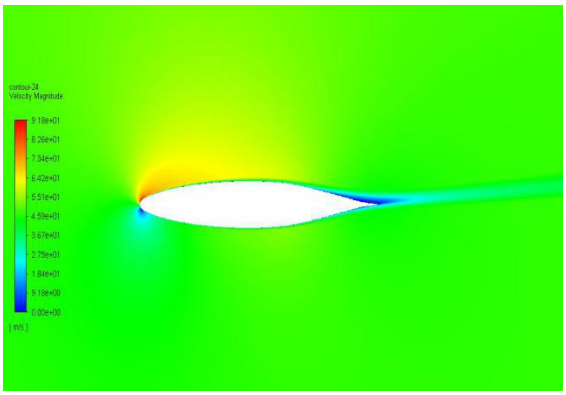

Fig. 20.b. 6º Symmetric airfoil velocity distribution(Fluent)

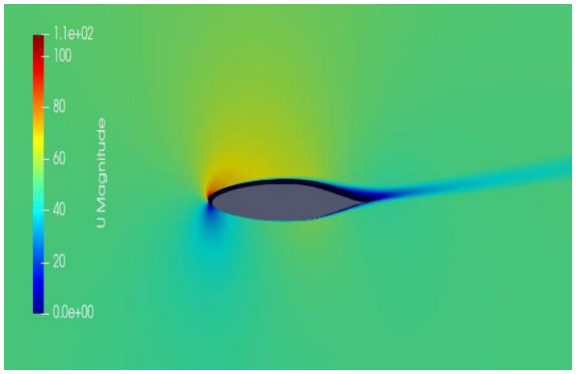

Fig. 21.a. 8º Symmetric airfoil velocity distribution(OpenFOAM)

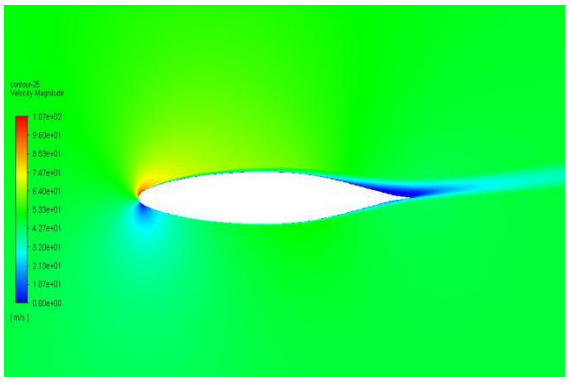

Fig. 21.b. 8º Symmetric airfoil velocity distribution(Fluent)

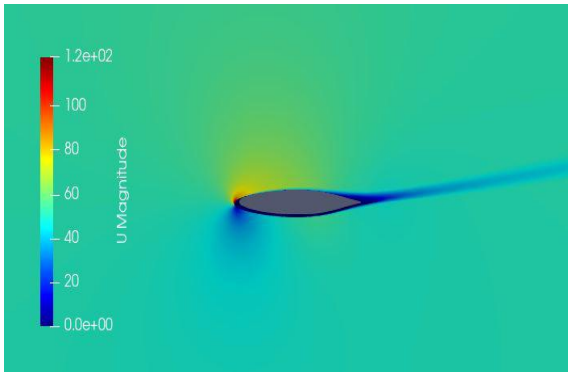

Fig. 22.a. 10º Symmetric airfoil velocity distribution(OpenFOAM)

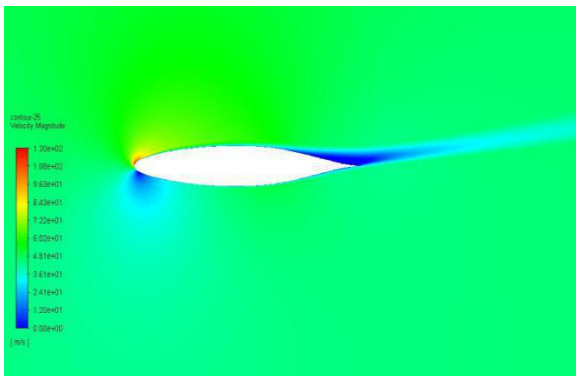

Fig. 22.b. 10º Symmetric airfoil velocity distribution(Fluent)

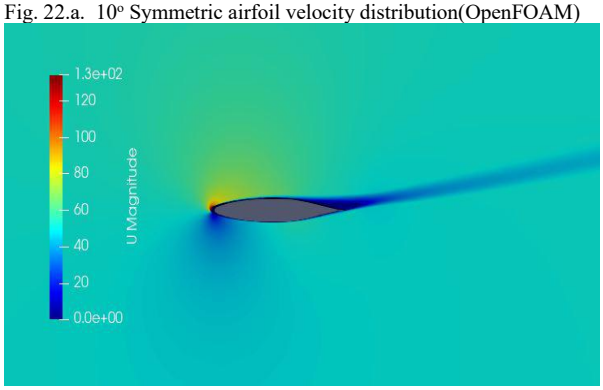

Fig. 23.a. 12º Symmetric airfoil velocity distribution(OpenFOAM)

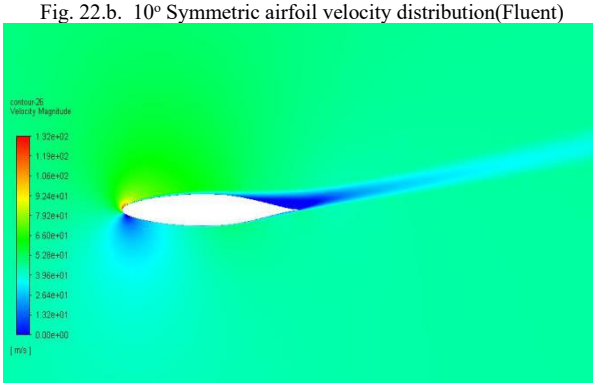

Fig. 23.b. 12º Symmetric airfoil velocity distribution(Fluent)

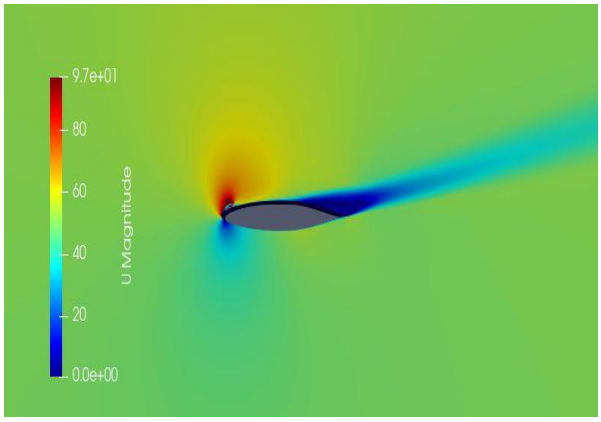

Fig. 24.a. 14º Symmetric airfoil velocity distribution(OpenFOAM)

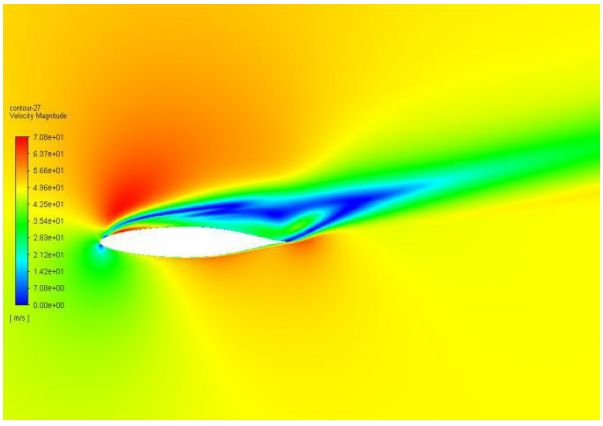

Fig. 24.b. 14º Symmetric airfoil velocity distribution(Fluent)

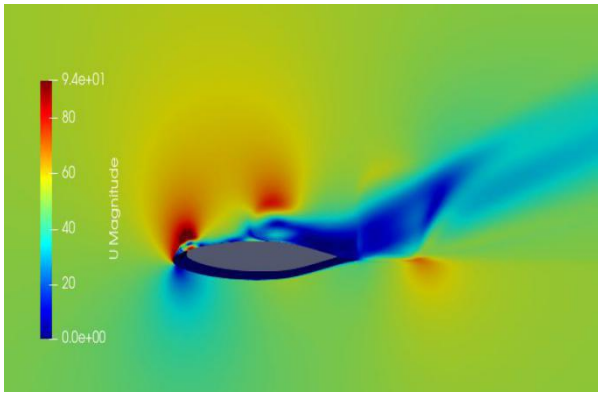

Fig. 25.a. 16° Symmetric airfoil velocity distribution(OpenFOAM)

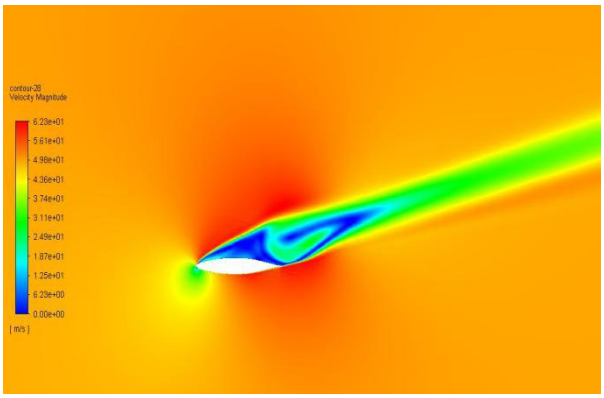

Fig. 25.b. 16° Symmetric airfoil velocity distribution(Fluent)

The lift and drag coefficient obtained from the simulation is given below for both OpenFOAM and ANSYS.

AOA	C_L	C_D
0	-0.00131631	0.0132359
2	0.194687	0.013957
4	0.387527	0.0155137
6	0.572088	0.0181673
8	0.741602	0.0220709
10	8.816379e-01	2.806280e-02
12	1.04018	0.0468949
14	0.754503551	0.144139165
16	0.785386123	0.199927121

Table. 4. Symmetric airfoil C_L and C_D values(OpenFOAM)

AOA	C_L	C_D
0	4.2869e-04	1.3054e-02
2	2.0252e-01	1.3417e-02
4	4.0009e-01	1.4483e-02
6	5.8629e-01	1.6364e-02
8	7.5159e-01	1.9474e-02
10	8.8779e-01	2.4601e-02
12	9.8180e-01	3.3378e-02
14	9.3156e-01	9.2609e-02
16	0.9012	0.098

Table. 5. Symmetric airfoil C_L and C_D values(Fluent)

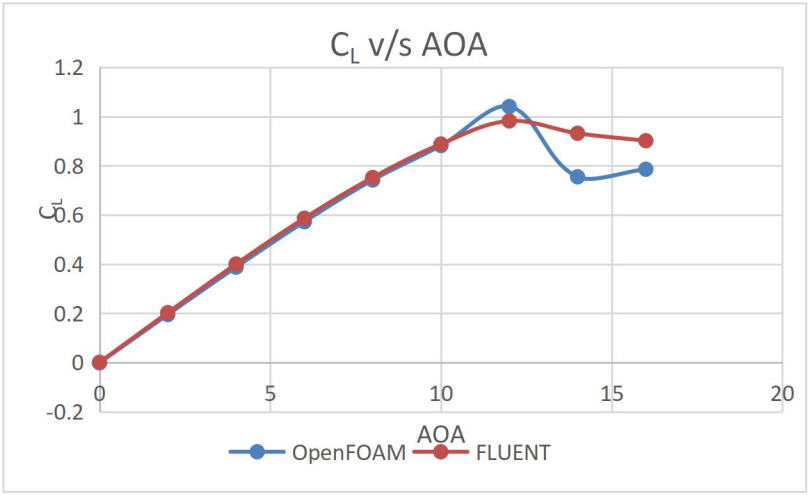

Fig. 26. Symmetric airfoil C_L v/s AOA

In symmetric airfoil, at lower angles of attack, the flow is smooth over the airfoil and there isn't much separation. But, as the angle of attack is increased, the flow separation starts happening leading to circulation. Due to this circulation, lift is produced. From the C_L v/ AOA and C_D v/ AOA curves plotted for the symmetric airfoil, it can be seen that as the angle is increased, both the lift and drag coefficient increase. There is a linear relationship between the AOA and C_L up until an angle of 10 degrees and above which the value increases rapidly and drops down. This sudden drop in C_L and increase in C_D is due to adverse separation of flow on the suction surface of the airfoil. The angle at which maximum C_L is attained is called the maximum angle of attack and for this symmetric airfoil, it is 12°. Any angle after this is called the stalling angle and the generation of lift reduces and drag increases.

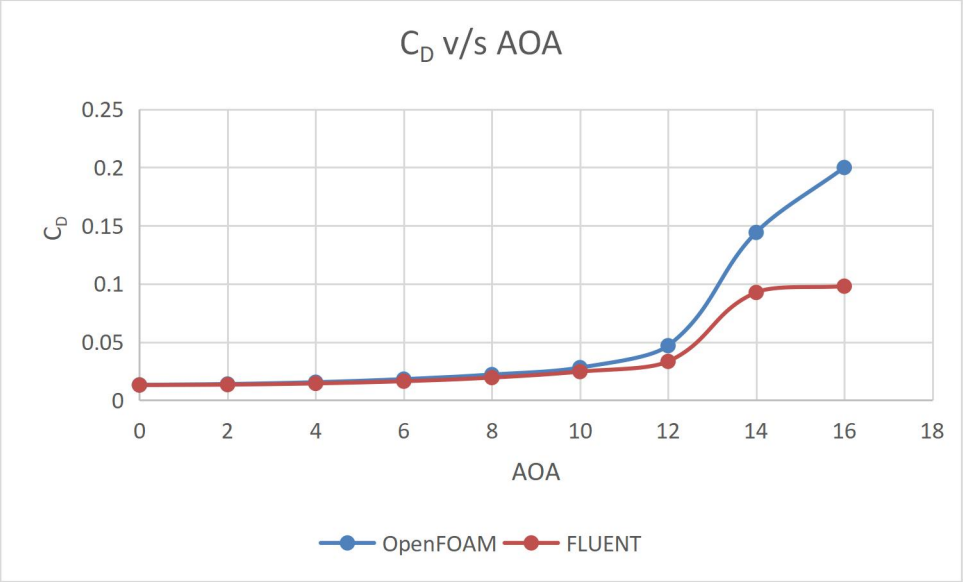

Fig. 27. Symmetric airfoil C_D v/s AOA

The pressure distribution plots obtained for cambered airfoil is presented below for both OpenFOAM and ANSYS.

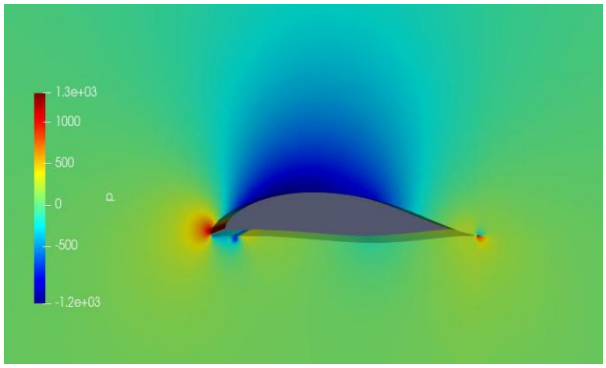

Fig. 28.a. 0° Cambered airfoil pressure distribution(OpenFOAM)

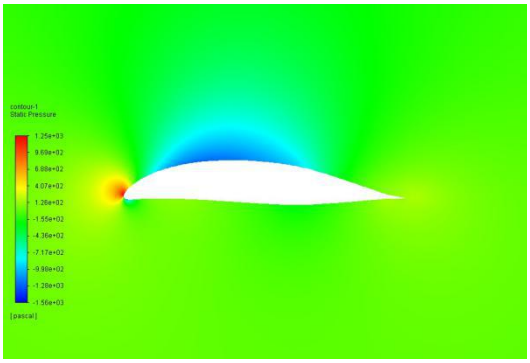

Fig. 28.b. 0° Cambered airfoil pressure distribution(Fluent)

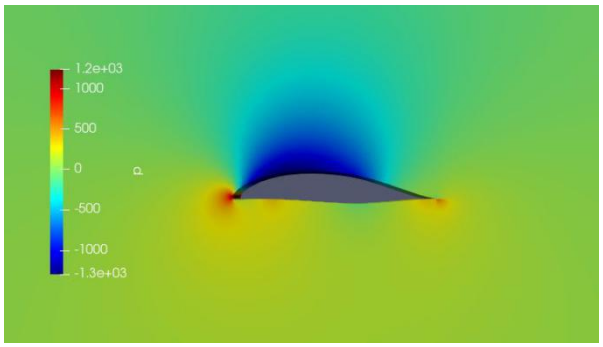

Fig. 29.a. 2º Cambered airfoil pressure distribution(OpenFOAM)

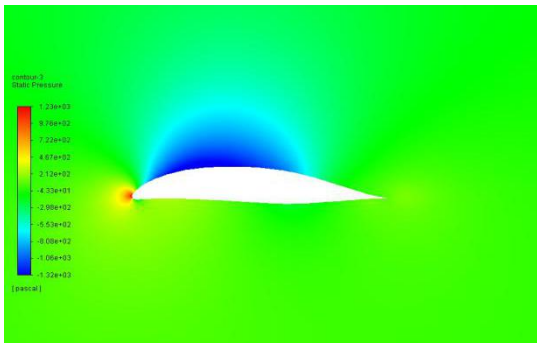

Fig. 29.b. 2º Cambered airfoil pressure distribution(Fluent)

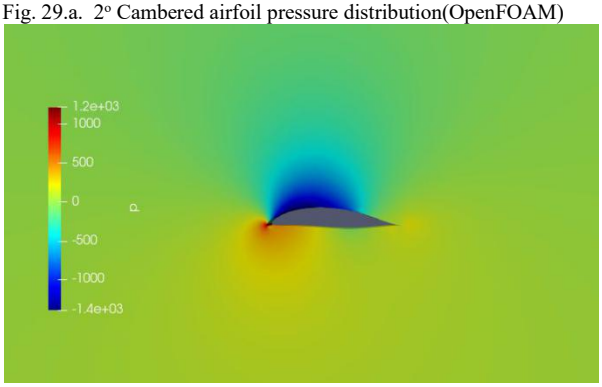

Fig. 30.a. 4º Cambered airfoil pressure distribution(OpenFOAM)

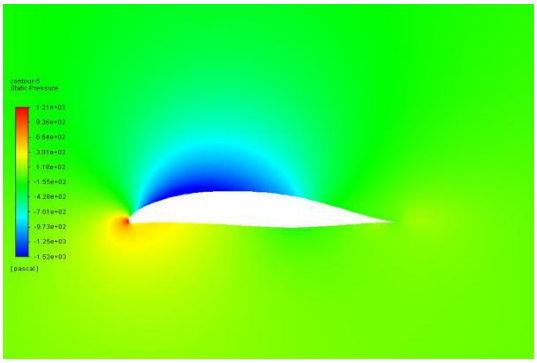

Fig. 30.b. 4º Cambered airfoil pressure distribution(Fluent)

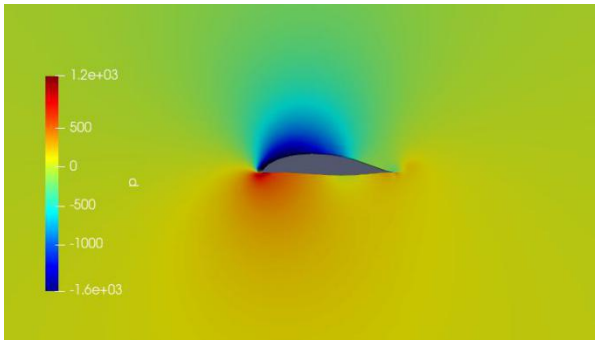

Fig. 31.a. 6º Cambered airfoil pressure distribution(OpenFOAM)

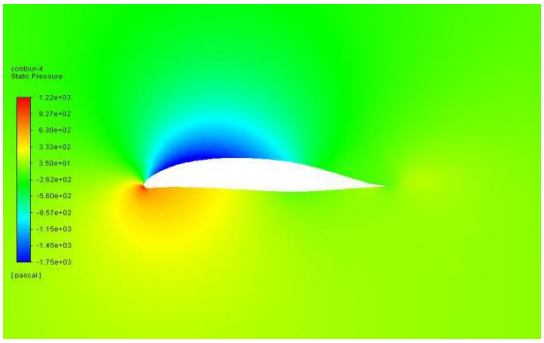

Fig. 31.b. 6º Cambered airfoil pressure distribution(Fluent)

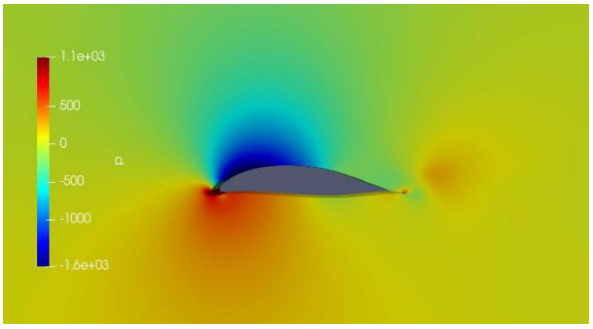

Fig. 32.a. 8º Cambered airfoil pressure distribution(OpenFOAM)

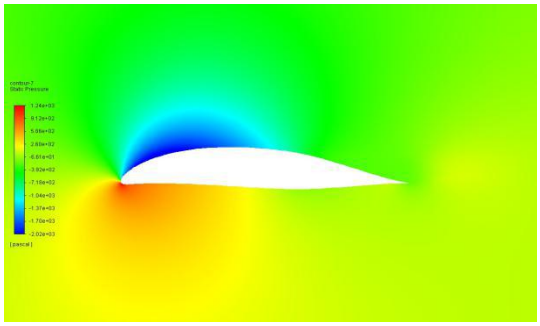

Fig. 32.b. 8º Cambered airfoil pressure distribution(Fluent)

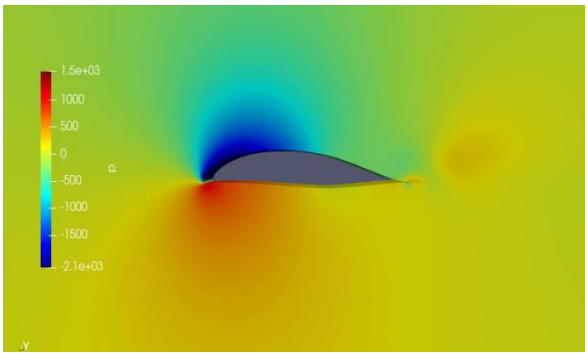

Fig. 33.a. 10º Cambered airfoil pressure distribution(OpenFOAM)

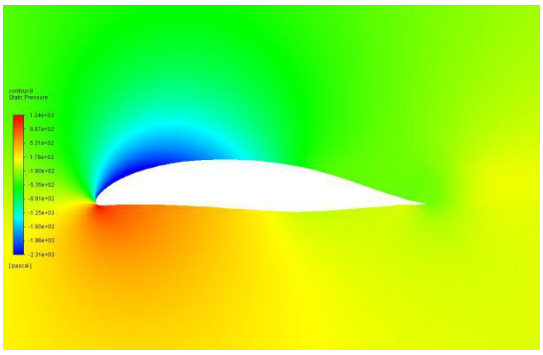

Fig. 33.b. 10º Cambered airfoil pressure distribution(Fluent)

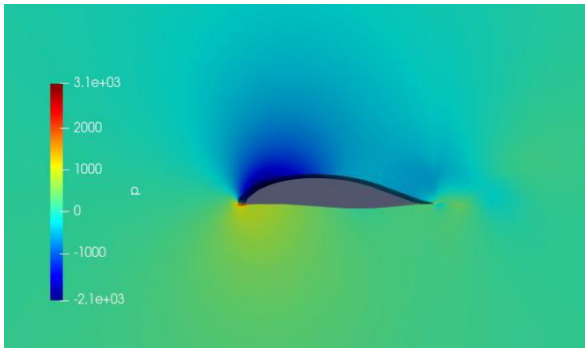

Fig. 34.a. 12º Cambered airfoil pressure distribution(OpenFOAM)

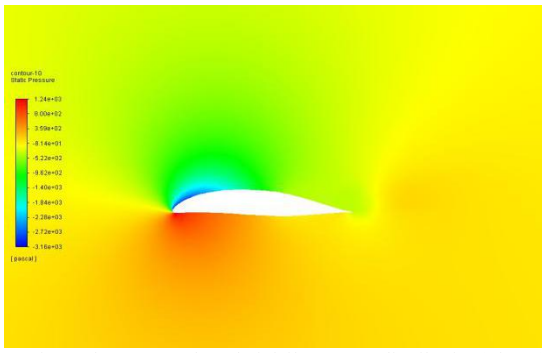

Fig. 34.b. 12º Cambered airfoil pressure distribution(Fluent)

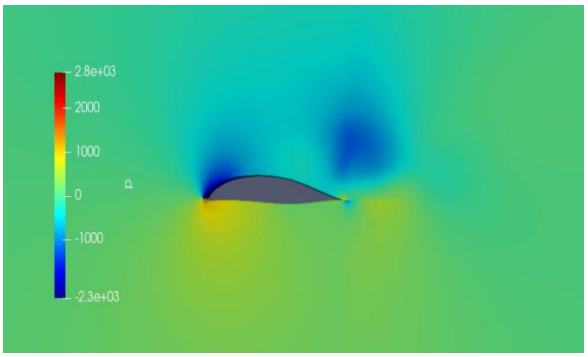

Fig. 35.a. 16º Cambered airfoil pressure distribution(OpenFOAM)

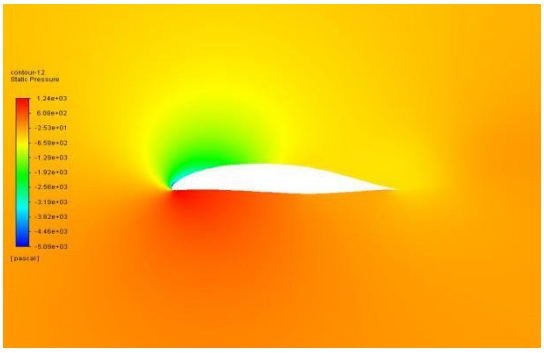

Fig. 35.b. 16º Cambered airfoil pressure distribution(Fluent)

The velocity distribution plots obtained for cambered airfoil is presented below for both OpenFOAM and ANSYS.

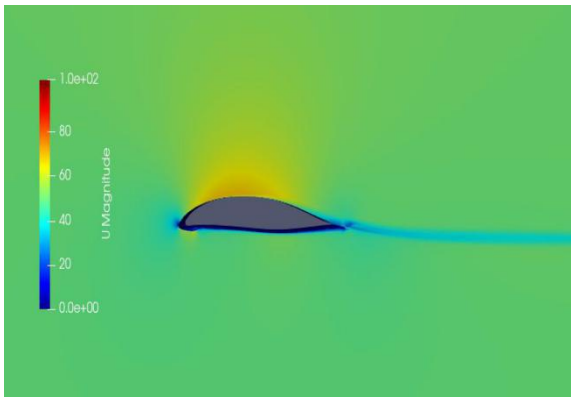

Fig. 36.a. 0º Cambered airfoil velocity distribution(OpenFOAM)

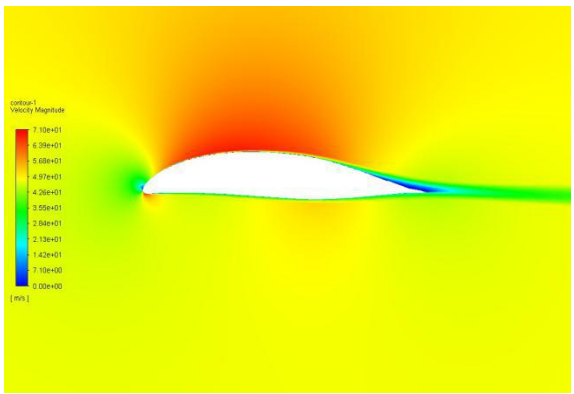

Fig. 36.b. 0º Cambered airfoil velocity distribution(Fluent)

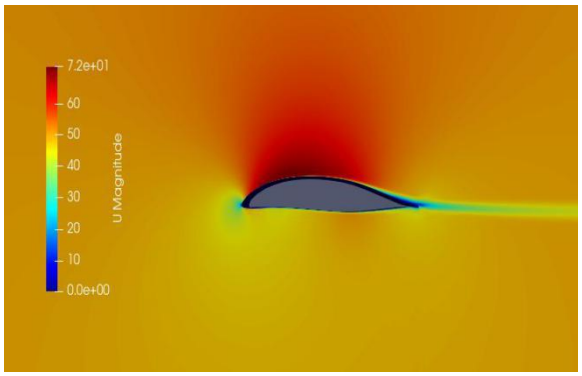

Fig. 37.a. 2º Cambered airfoil velocity distribution(OpenFOAM)

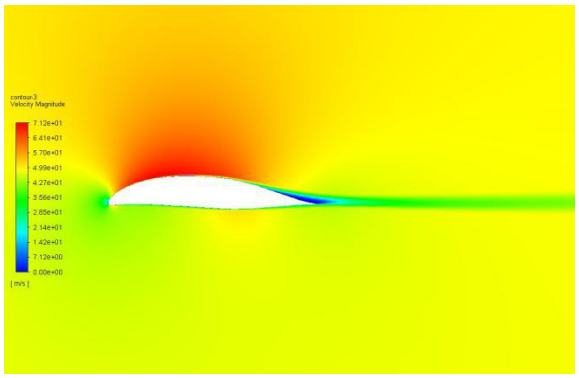

Fig. 37.b. 2º Cambered airfoil velocity distribution(Fluent)

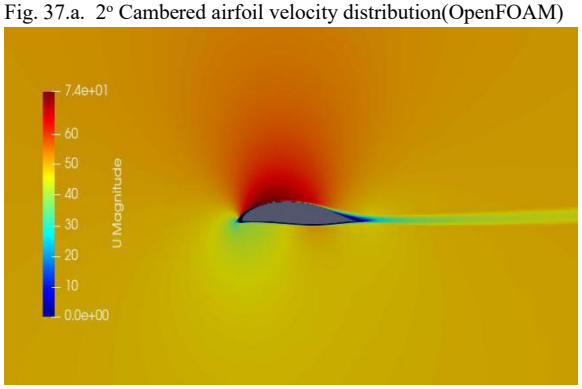

Fig. 38.a. 4º Cambered airfoil velocity distribution(OpenFOAM)

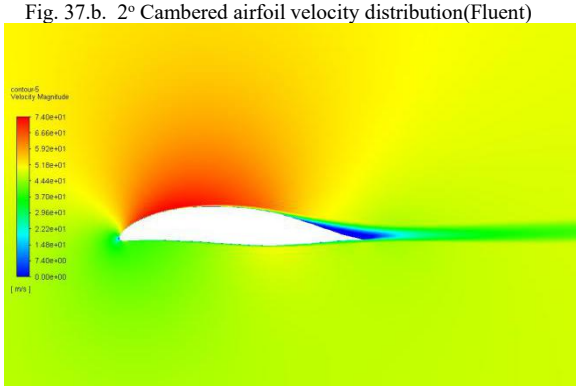

Fig. 38.b. 4º Cambered airfoil velocity distribution(Fluent)

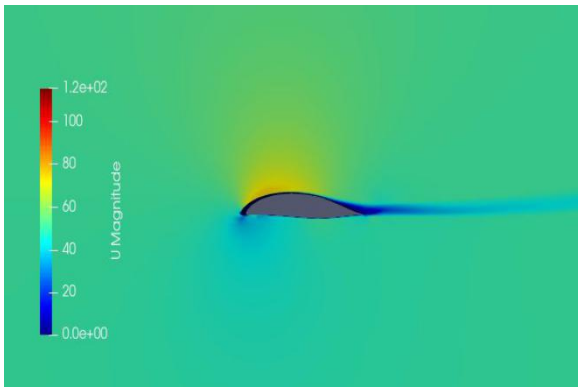

Fig. 39.a. 6º Cambered airfoil velocity distribution(OpenFOAM)

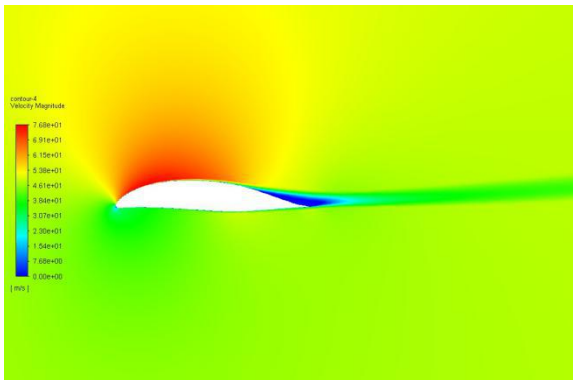

Fig. 39.b. 6º Cambered airfoil velocity distribution(Fluent)

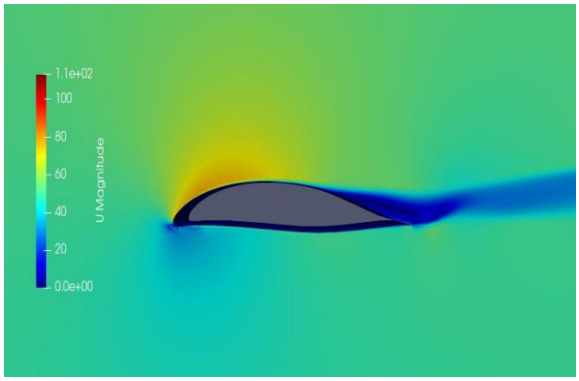

Fig. 40.a. 8º Cambered airfoil velocity distribution(OpenFOAM)

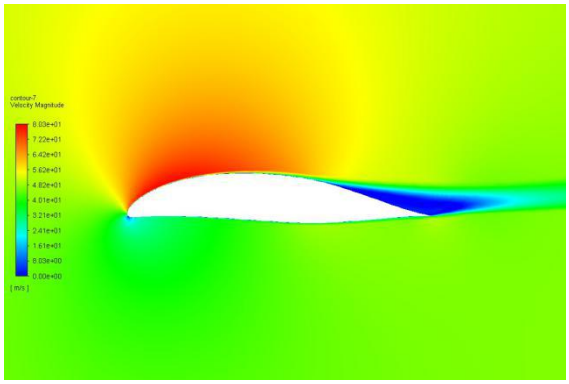

Fig. 40.b. 8º Cambered airfoil velocity distribution(Fluent)

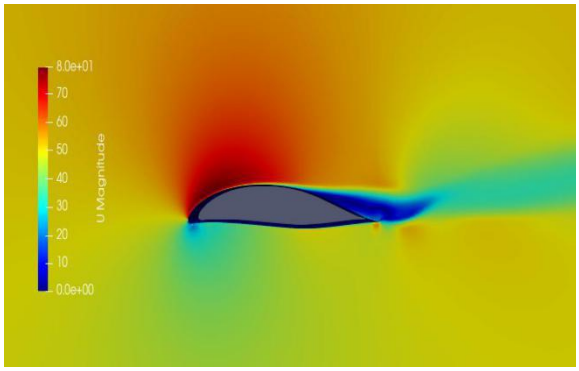

Fig. 41.a. 10º Cambered airfoil velocity distribution(OpenFOAM)

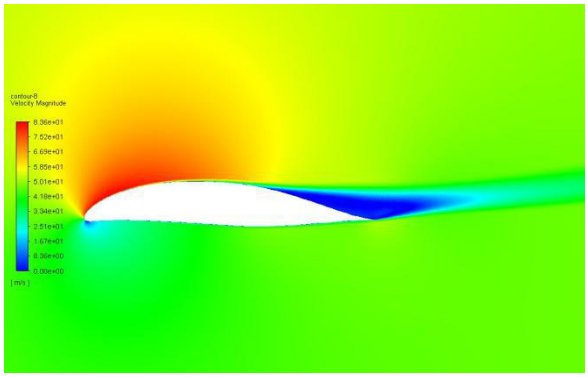

Fig. 41.b. 10º Cambered airfoil velocity distribution(Fluent)

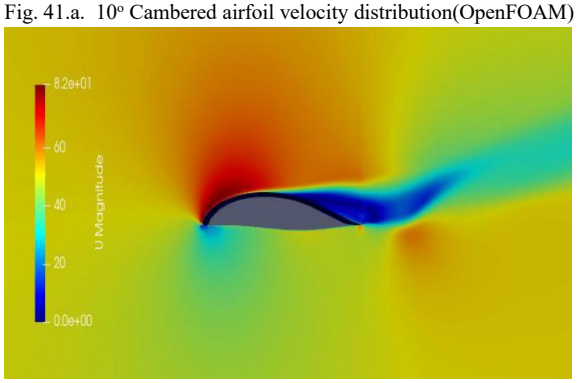

Fig. 42.a. 12º Cambered airfoil velocity distribution(OpenFOAM)

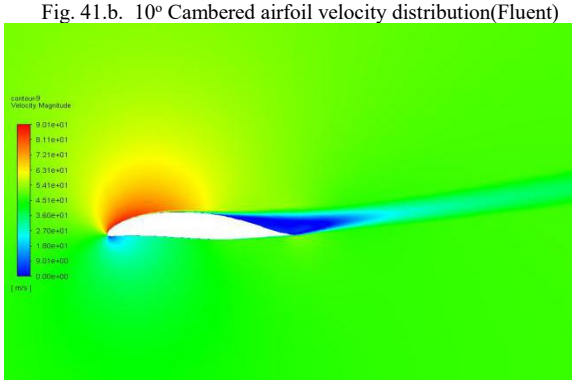

Fig. 42.b. 12º Cambered airfoil velocity distribution(Fluent)

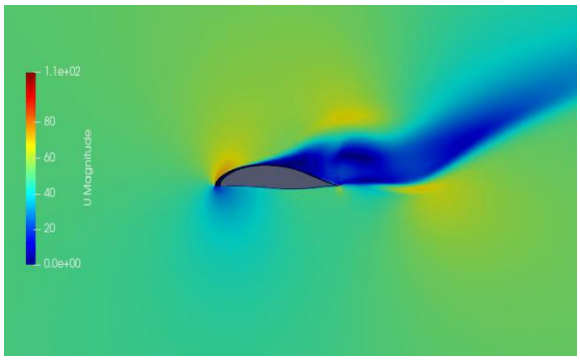

Fig. 43.a. 16º Cambered airfoil velocity distribution(OpenFOAM)

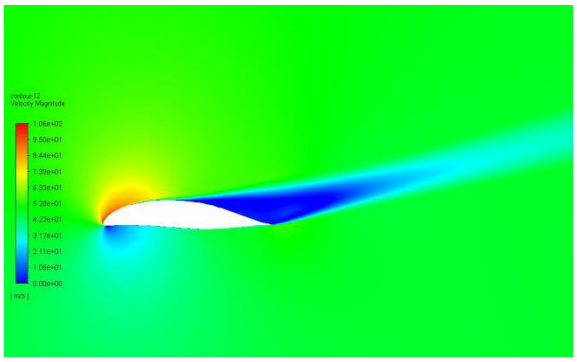

Fig. 43.b. 16º Cambered airfoil velocity distribution(Fluent)

AOA	C_L	C_D
0	0.56109	1.80602e-02
2	7.950521e-01	2.392626e-02
4	8.416306e-01	2.343645e-02
6	1.137980e+00	2.653878e-02
8	1.177270e+00	2.349830e-02
10	1.207581e+00	4.053571e-02
12	1.247648e+00	1.649258e-01
16	1.033336e+00	1.666331e-01

Table. 6. Cambered airfoil C_L and C_D values(OpenFOAM)

In the cambered airfoil, it can be seen that at zero angle of attack there is significant lift being produced, unlike the symmetric airfoil. Thus, for the cambered airfoil to produce zero lift it must be placed at a negative angle of attack. This angle of attack is called the zero angle of attack. As the angle is increased, the C_L and C_D value increases. In this study, the cambered airfoil attains a maximum C_L at AOA of 16º. The values obtained by OpenFOAM is almost comparable to that attained by fluent. The C_D value increases suddenly in the OpenFOAM at AOA of 12º. Compared to symmetric airfoils, cambered airfoils have a larger angle of function

as stalling occurs much later in them whereas in symmetric airfoil stall occurs at a much lower AOA.

AOA	C_L	C_D
0	4.7096e-01	1.6161e-02
2	6.4405e-01	1.8275e-02
4	8.0248e-01	2.1332e-02
6	9.4157e-01	2.6254e-02
8	1.0616e+00	3.2816e-02
10	1.1636e+00	4.1038e-02
12	1.2455e+00	5.1489e-02
16	1.3068e+00	8.5899e-02

Table. 7. Cambered airfoil C_L and C_D values(Fluent)

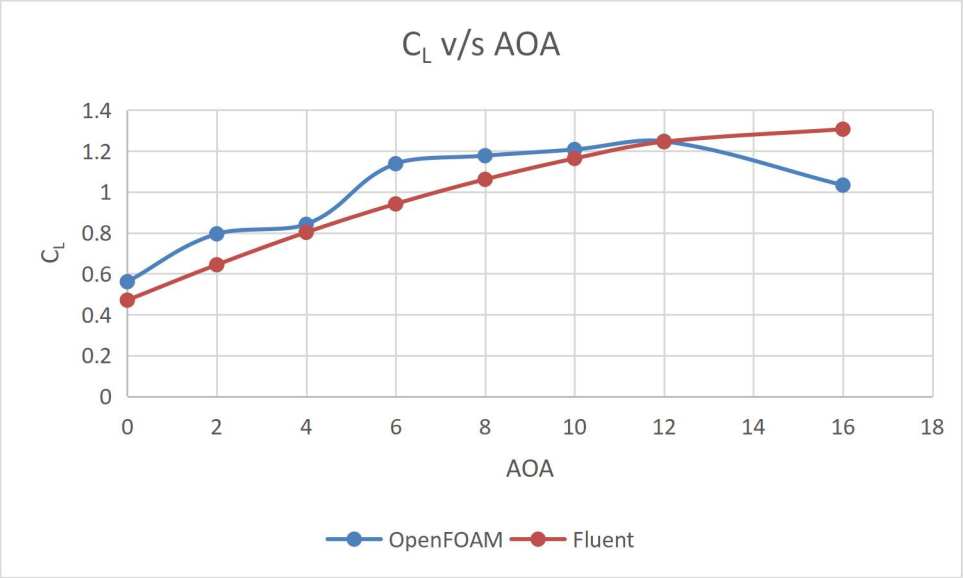

Fig. 44. Symmetric airfoil C_L v/s AOA

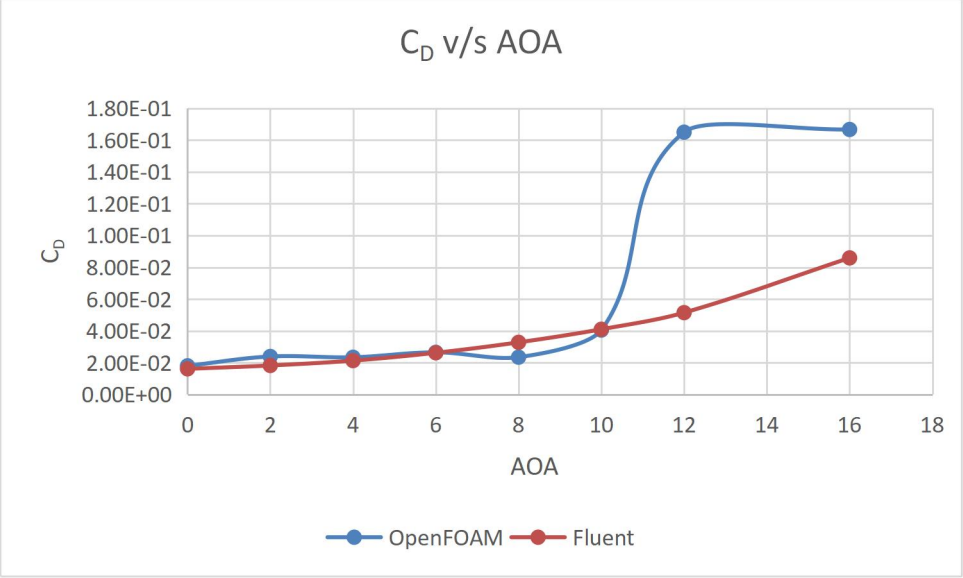

Fig. 45. Symmetric airfoil C_D v/s AOA

The above contours of pressure and velocity for both symmetric and cambered airfoils show that with an increase in angle of attack the boundary layer tends to separate from the surface of the airfoil. At one particular angle, the separation is so large that it leads to a decrease in the lift produced by the airfoil. A comparison study of the results obtained from symmetric and cambered NACA 66_2-015 airfoils was done and they are shown below. It can be seen that cambered airfoil has a higher C_L and C_D value compared to the symmetric airfoil.

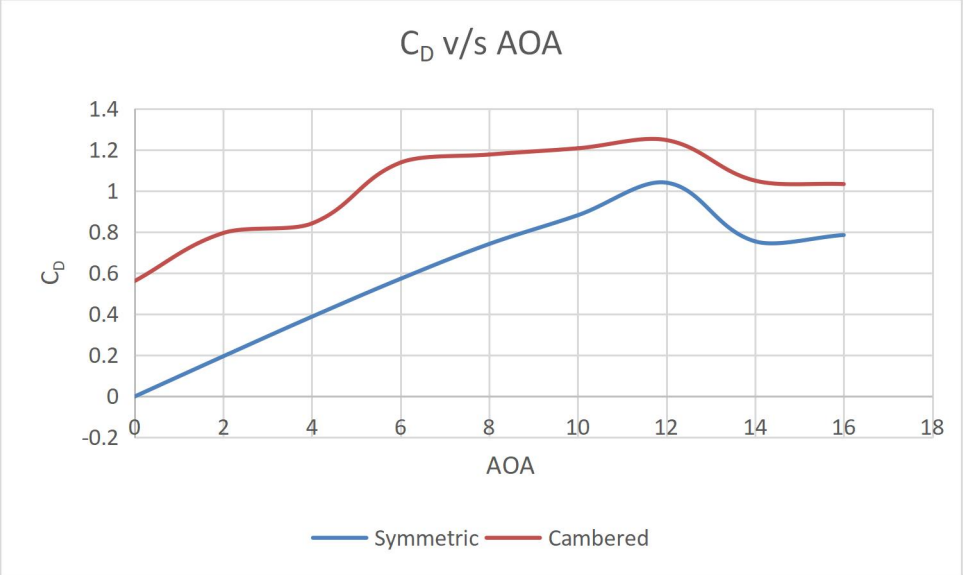

Fig. 46. Symmetric and cambered airfoil C_L v/s AOA

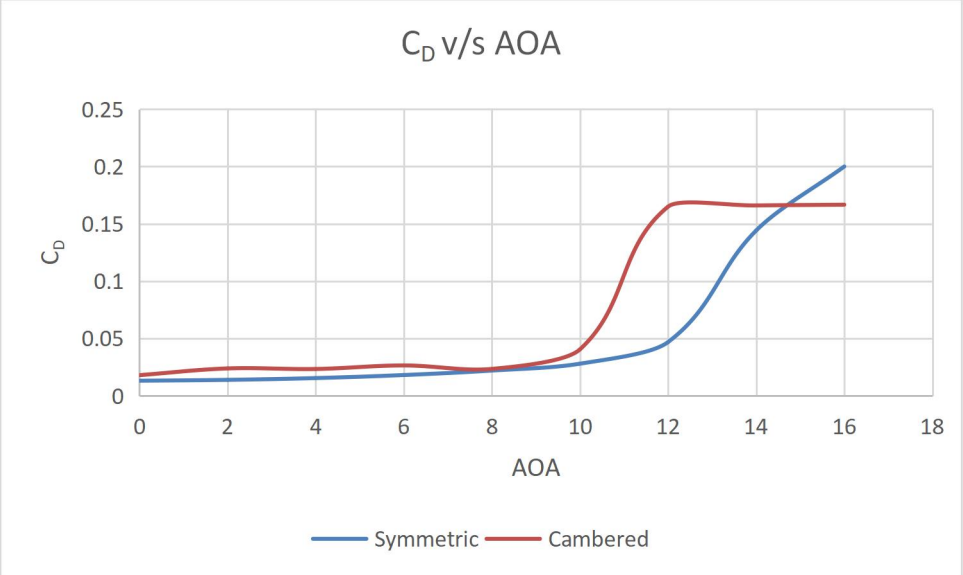

Fig. 47. Symmetric and cambered airfoil C_D v/s AOA

Also, it is seen that the drag coefficient obtained in OpenFOAM vary too much with respect to the results obtained by ANSYS Fluent. Especially for the cambered airfoil. The variation of the drag coefficient increases rapidly as the AOA is increased for both the airfoils.

References

[1] https://encyclopedia2.thefreedictionary.com/airfoil+classification#:~:text=Airfoils%20are%20divided%20into%20three,and%20well%2Drounded%20leading%20edges.

[2] https://en.wikipedia.org/wiki/Airfoil

[3] https://www.cfd-online.com/Wiki/SIMPLE_algorithm

[4] https://www.openfoam.com/documentation/user-guide/turbulence.php

[5] https://www.openfoam.com/documentation/guides/latest/doc/verification-validation-turbulent-flat-plate-zpg.html

[6] https://www.openfoam.com/documentation/guides/latest/doc/verification-validation-naca0012-airfoil-2d.html

[7] Fundamentals of Aerodynamics Fifth Edition John D. Anderson, Jr.

[8] THEORY OF WING SECTIONS Including a Summary of Airfoil Data, Ira H. Abbott and Albert E. Von Doenhoff

[9] "Comparative Assessment of Drag & Lift Force on NACA 66(2)-015 Airfoil Model by Computational Fluid Dynamics and Experimental Method" Prasad Kallolimath, Mayur Anvekar, International Journal of Engineering Research & Technology (IJERT), ISSN: 2278-0181, Vol. 7 Issue 07, July-2018